A MONTE CARLO TECHNIQUE USING A FAST REPETITIVE ANALOG COMPUTER FOR DETERMINING LOWEST EIGENVALUES OF PARTIAL DIFFERENTIAL EQUATIONS FOR VARIOUS BOUNDARIES WITH APPLICATIONS

by

Richard T. D'Aquanni

A Thesis Submitted to the Faculty of the

DEPARTMENT OF ELECTRICAL ENGINEERING

In Partial Fulfillment of the Requirements
For the Degree of

MASTER OF SCIENCE

In the Graduate College

THE UNIVERSITY OF ARIZONA

1970

STATEMENT BY AUTHOR

This thesis has been submitted in partial fulfillment of requirements for an advanced degree at The University of Arizona and is deposited in the University Library to be made available to borrowers under rules of the Library.

Brief quotations from this thesis are allowable without special permission, provided that accurate acknowledgment of source is made. Requests for permission for extended quotation from or reproduction of this manuscript in whole or in part may be granted by the head of the major department or the Dean of the Graduate College when in his judgment the proposed use of the material is in the interests of scholarship. In all other instances, however, permission must be obtained from the author.

SIGNED: 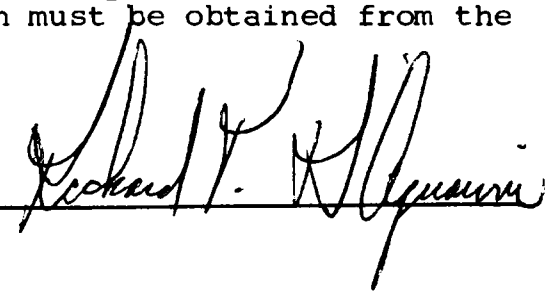

APPROVAL BY THESIS DIRECTOR

This thesis has been approved on the date shown below:

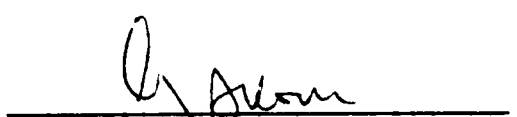

G. A. Korn
Professor of Electrical Engineering

4/30/69
Date

ACKNOWLEDGMENTS

The author is indebted to Professor Granino A. Korn for his knowledgeable suggestions and direction, to Dr. Howard Handler for both his uncovering and preliminary implementation of this method, and to Professor D. Dudley for his useful comments.

TABLE OF CONTENTS

LIST OF ILLUSTRATIONS

LIST OF TABLES

ABSTRACT

This paper describes a Monte Carlo technique for estimating the lowest eigenvalues of certain elliptic and hyperbolic partial differential equations with Dirichlet boundary conditions.[10] A stochastic process whose output conditional probability density distribution satisfies a partial differential equation similar to the partial differential equation under consideration is, along with the boundary conditions, implemented on ASTRAC II, a fast repetitive analog computer.

Eight different boundaries on the scalar Helmholtz equation in one, two, and three-dimensional space were implemented. Each of the resulting eight lowest-eigenvalue estimates is then compared to its corresponding and expected true lowest eigenvalue. Computer hardware errors, along with the error resulting from the mathematical approximation employed in deriving the estimate, are indicated. Corrective measures are included when necessary. Applications result from a presentation of analogies relating the partial differential equations under consideration to partial differential equations modeling physical processes.

INTRODUCTION

Numerical solutions for the lowest eigenvalues of certain partial differential equations are sometimes difficult to determine if one employs standard numerical techniques. A list of these standard techniques should include the finite difference method, Galerkin's method and the energy method of Rayleigh-Ritz.[12] Less standard, yet more sophisticated when applied to specific problems, are the methods of point matching or collocation,[13,15] segment matching,[14] and conformal mapping.[1,2]

A Monte Carlo method applied to lowest-eigenvalue estimation has been introduced and mathematically illustrated by Donsker and Kac.[5] Theoretically, Donsker and Kac suggested generation of a stochastic process (represented by generalized Langevin equations) resulting from the application of a white-Gaussian-noise forcing function to a first-order system, (see Appendix A). The conditional probability density function of the output variable (which completely describes the output process, since it is a first-order Markov process) satisfies Kolmogorov's backward partial differential equation. The determination of eigenvalues of various deterministic differential equations is based on these Kolmogorov backward partial differential equations.

In this paper, a stochastic process is generated and applied in the estimation of the lowest eigenvalues of

the scalar Helmholtz equation for a number of geometric one, two and three-dimensional boundaries representing the bodies under consideration. Realizing that randomness, the basis of Monte Carlo Methods, requires many repetitions for accurate and consistent estimates, we turn to the computer as the only feasible means to implement such a process. The computer to be employed is the second in a series of Arizona Statistical Repetitive Analog Computers, ASTRAC II.[11,14]

EXAMPLE PROBLEM

The implementation of one typical problem in detail will illustrate the Monte Carlo Technique employed. The sampling procedure and formula constituting the technique are common to all eigenvalue problems considered in this paper.

The problem considered is that of determining the lowest eigenvalue of a vibrating string. The linear partial differential equation governing small transverse vibrations of an elastic string under fixed constraints is:[3]

$$\frac{\partial^2 U(x,t)}{\partial x^2} = \frac{\partial^2 U(x,t)}{\partial t^2} \qquad (1)$$

where $U(x,t)$ is the transverse vibration amplitude at position x at time t, and where the normally encountered coefficient $c^2 = T/\rho$ has been normalized to unity through a linear transformation in the x coordinate.

The boundary conditions on Eq. (1) will be taken as

$$\begin{aligned} U(-10,t) &= 0 \\ U(10,t) &= 0 \end{aligned} \qquad (t \geq 0) \qquad (2)$$

and the initial condition is

$$U(x,0) = f(x) \qquad (-10 \leq x \leq 10) \qquad (3)$$

The classical solution to Eq. (1) with boundary conditions given by Eq. (2) can be found by first separating variables, assuming

$$U(x,t) = X(x)T(t) \tag{4}$$

which, when substituted into Eq. (1) yields

$$X''(x) + k_i^2 X(x) = 0 \tag{5}$$

$$T''(t) + k_i^2 T(t) = 0 \tag{6}$$

where $k_i^2 = \frac{-X''(x)}{X(x)} = \frac{-T''(t)}{T(t)}$ is an arbitrary constant.

The nontrivial solution to Eq. (5) is

$$X(x) = A \cos k_i x + B \sin k_i x \tag{7}$$

which satisfies the Eq. (2) boundary conditions when

$$k_i^2 = \left(\frac{i\pi}{20}\right)^2 \tag{8}$$

Hence, the lowest eigenvalue k_1^2 or λ^1 satisfying Eq. (1) and Eq. (2) is

$$k_1^2 = \left(\frac{\pi}{20}\right) \tag{9}$$

Kolmogorov's stochastic partial differential equation is given as

$$G^2 Dn \frac{\partial^2 p(x,t/x_o,0)}{\partial x^2} = \frac{\partial p(x,t/x_o,0)}{\partial t} \qquad (10)$$

where $p(x,t/x_o,0)$ is the conditional probability density of the Markov process represented by random variable x. Introducing the normalized time variable

$$T = \frac{t}{G^2 Dn}$$

Eq. (10) may be written as

$$\frac{\partial^2 p(x,T/x_o,0)}{\partial x^2} = \frac{\partial p(x,T/x_o,0)}{\partial T} \qquad (11)$$

Boundary conditions for Eq. (11) are given as

$$\begin{aligned} p(-10,T/x_o,0) &= 0 \\ & \qquad (T \geq 0) \qquad (12) \\ p(10,T/x_o,0) &= 0 \end{aligned}$$

with

$$p(x,T/x_o,0) = \delta(x - x_o) \qquad (-10 \leq x_o \leq 10) \quad (13)$$

as the initial condition.

The classical solution to Eq. (11) with boundary conditions given as Eq. (12) is achieved by again first separating variables, assuming

$$p(x,T/x_o,0) = X(x)V(T) \tag{14}$$

which when substituted into Eq. (11) yields

$$X''(x) + k_i^2 X(x) = 0 \tag{15}$$

$$V'(T) + k_i^2 V(T) = 0 \tag{16}$$

where $k_i^2 = -\frac{X''(x)}{X(x)} = -\frac{V'(T)}{V(T)}$ is an arbitrary constant.

The two space-dependent, second-order Helmholtz equations Eq. (5) and Eq. (15) are equal so that a solution to Eq. (15) resulting from Kolmogorov's stochastic partial differential equation will provide a solution to Eq. (5) resulting from the vibrating string deterministic partial differential equation for the given equal boundary conditions, Eq. (2) and Eq. (12).

The general solution to Eq. (11), formed by multiplying the general solution of Eq. (15) by the general solution of Eq. (16), is

$$p(x,T/x_o,0) = \sum_{i=1}^{\infty} F_i \left[\sin k_i x + \cos k_i x \right] e^{-k_i^2 T} \qquad (17)$$

To satisfy the boundary conditions of Eq. (12) we substitute Eq. (8) into Eq. (17) which then becomes

$$p(x,T/x_o,0) = \sum_{i=1}^{\infty} F_i \left[\sin\left(\frac{i\pi}{20}\right)x + \cos\left(\frac{i\pi}{20}\right)x \right] e^{-\left(\frac{i\pi}{20}\right)^2 T} \qquad (18)$$

Theoretically as $T \to \infty$, the most significant term in Eq. (18) occurs at $i = 1$, indicating that the dominating value for k_i^2 in Eq. (18) as $T \to \infty$ is the lowest eigenvalue for the vibrating string given by Eq. (9). A very large T value is computationally impractical and another method using two reasonably large T values is shown to provide similar results yielding a lowest eigenvalue solution for Eq. (18). This method and a more rigorous mathematical coverage from start to completion are given in Appendix A resulting in the following estimate for any lowest eigenvalue, λ^1:

$$\lambda^1 = \frac{\ln \frac{N_{t_1}}{N_{t_2}}}{t_2 - t_1} \qquad (19)$$

where N_{t_i} is the number of walks which remain within the specified boundaries during the real time interval $(0,t_i)$ or normalized time interval $(0,T_i)$ and N_{t_i} is calculated from the number of walks absorbed out of the total number of walks completed. Both these quantities are computer simulation outputs as discussed below.

The computer block diagram for the above example problem is given in Fig. 1. First observe the zero-mean (capacitor-coupled) one-dimensional Gaussian distributed random walk resulting from the integration of a binomially distributed random square wave. N(T), the random square wave has a variance 2Dn empirically measured as 30×10^{-6} $volts^2/sec.$ (16,10)

Transitions in the amplitude of N(T) may occur only at times specified by the noise clock frequency used to drive the random noise generator. It is important to note that the random walk's smallest step size $y(\Delta T)$ is a function of the noise clock frequency, the amplitude of the random square wave and the integrator gain G or 1/RC. Next, observe how random walk excursions beyond either the + 10 volt or - 10 volt fixed string boundaries are detected by use of two fast-analog comparators. The logic gates and flip-flop following the comparators are necessary for re-setting integrator and hence walk initial conditions. Finally, observe the binary counters and associated logic

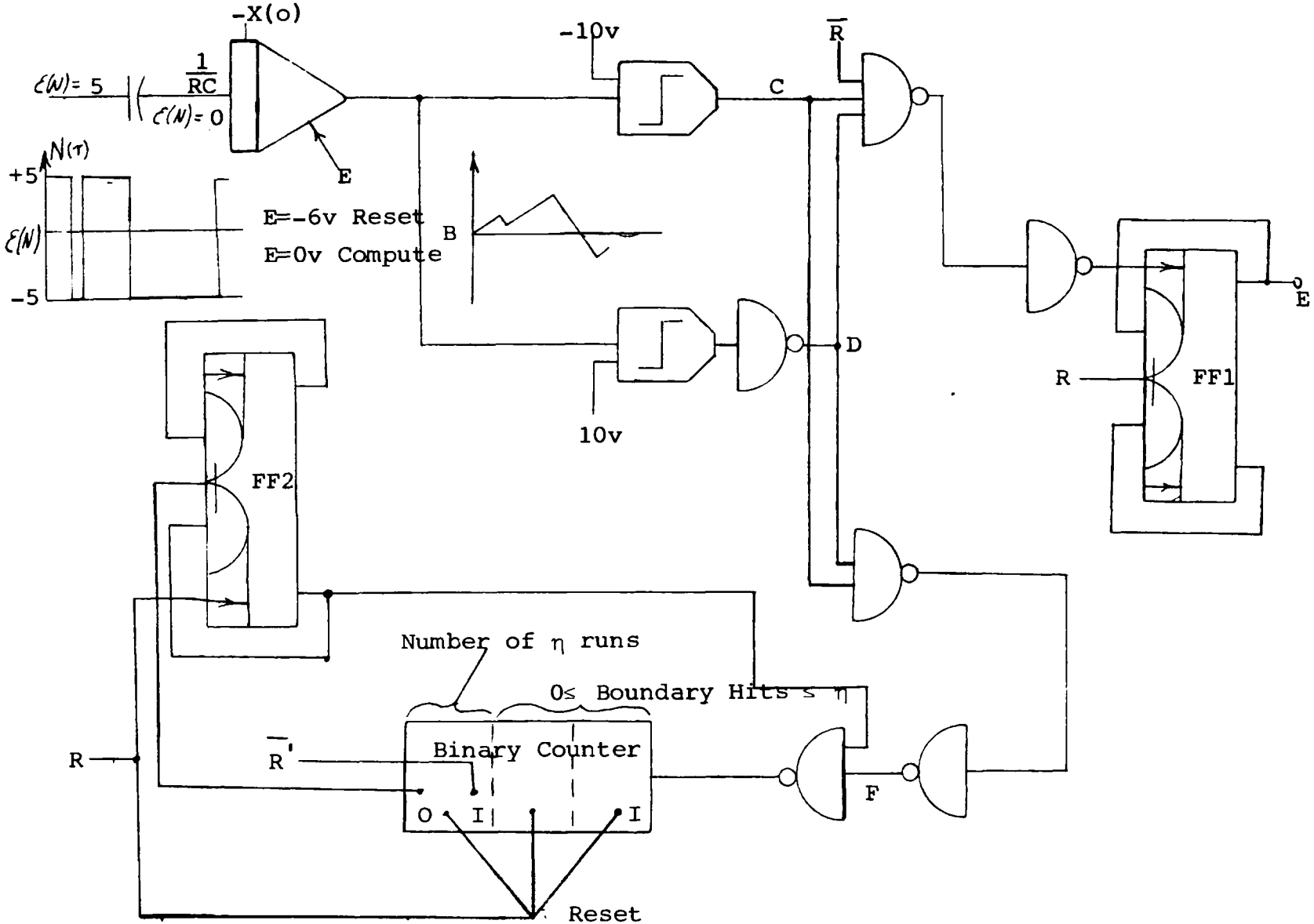

Figure 1. Implementation of One-Dimensional Vibrating String Example

used in tallying both the number of walks completed and the number of walks resulting in boundary absorption corresponding to total walk time, "T ".

Typical waveforms appearing in the simulation are given in Fig. 2. Figure 2A illustrates the basic timing pulse R which sets the repetition rate and the length of the random walks. T may be varied by similarly varying the duty cycle of R.

In Figure 2B, the random walk is shown along with the absorption boundary levels, $\pm$ 10 volts. In the first frame of the diagram, an absorption at the + 10 volt boundary has occurred. In the second frame, no absorption has occurred during the time interval allotted for the walk, and the signal is reset at the end of this interval marked by R. In the third frame, the signal has reached the - 10 volt level; the walk stops at this point and the integrator is reset to its starting position once again. Figures 2C and 2D show the comparator outputs which correspond to a + 10 volt and - 10 volt absorption, respectively. Figure 2E shows the integrator mode timing signal corresponding to the signals shown in Figs. 2B, 2C and 2D.

Figure 2F indicates the pulses inputted to the binary counter corresponding again to Fig. 2B, 2C and 2D. Figure 2G indicates waveform R' which controls the number of repetitions and time between repetitions.

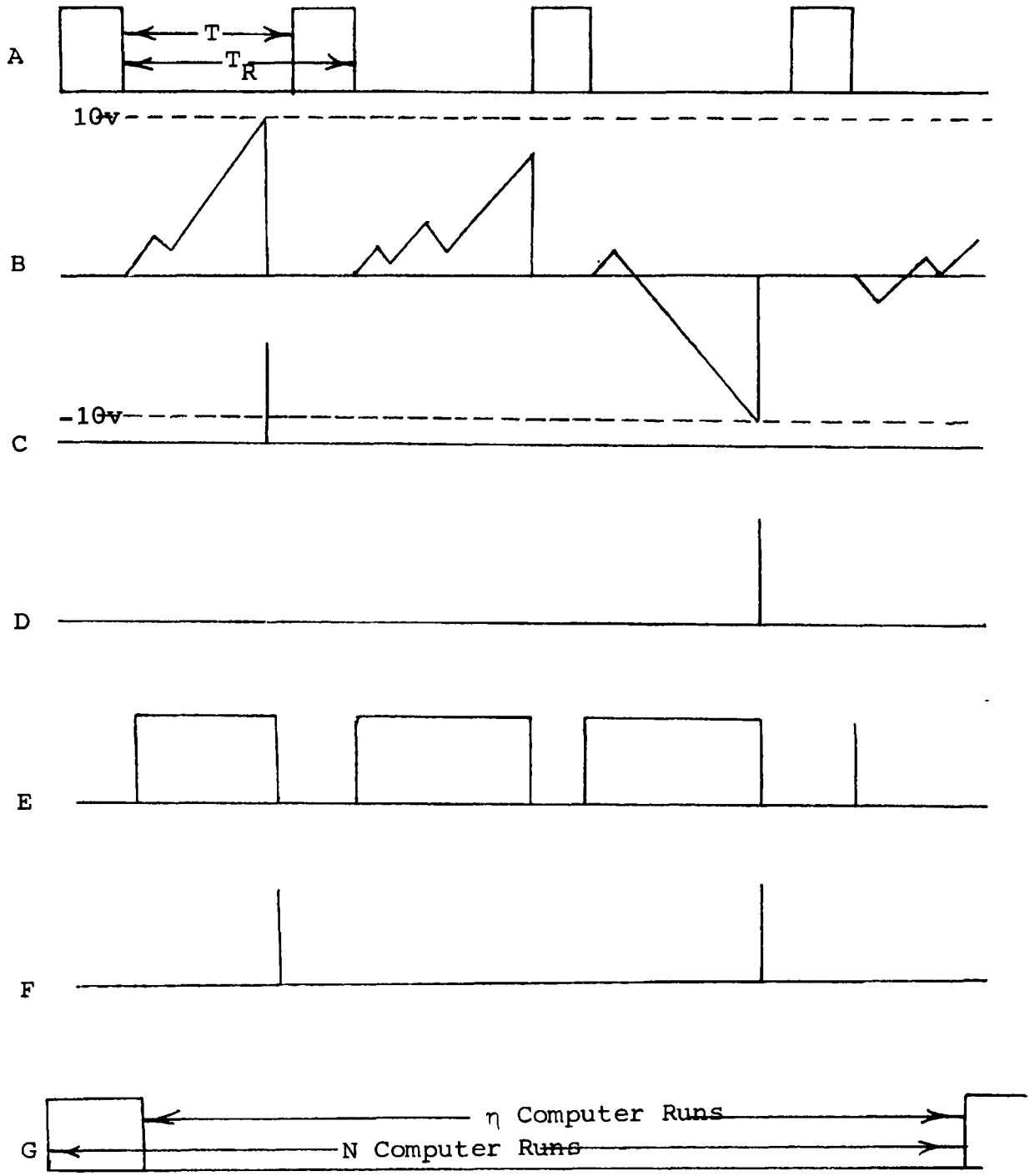

Figure 2. Typical Wave Forms

In general, the dimensionality of the boundary or describing partial differential equation would require just that many independent noise sources with boundaries for each variable. Implementation of two and three dimensional boundaries are illustrated in Figs. 3A and 3B respectively.

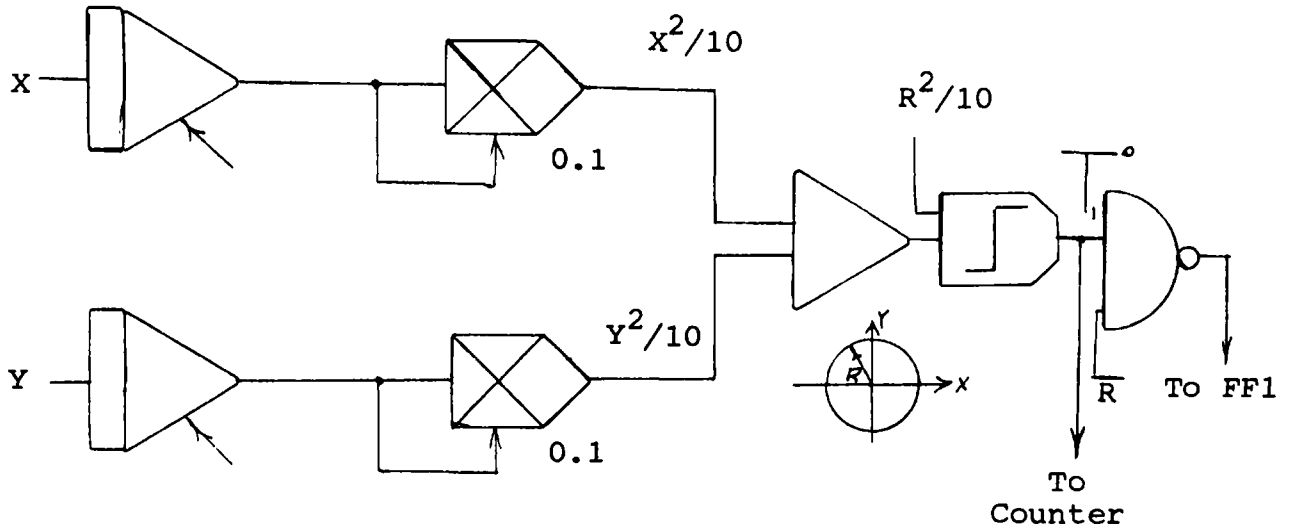

A. Two-Dimensional Circular Membrane

B. Three-Dimensional Cylindrical Boundary

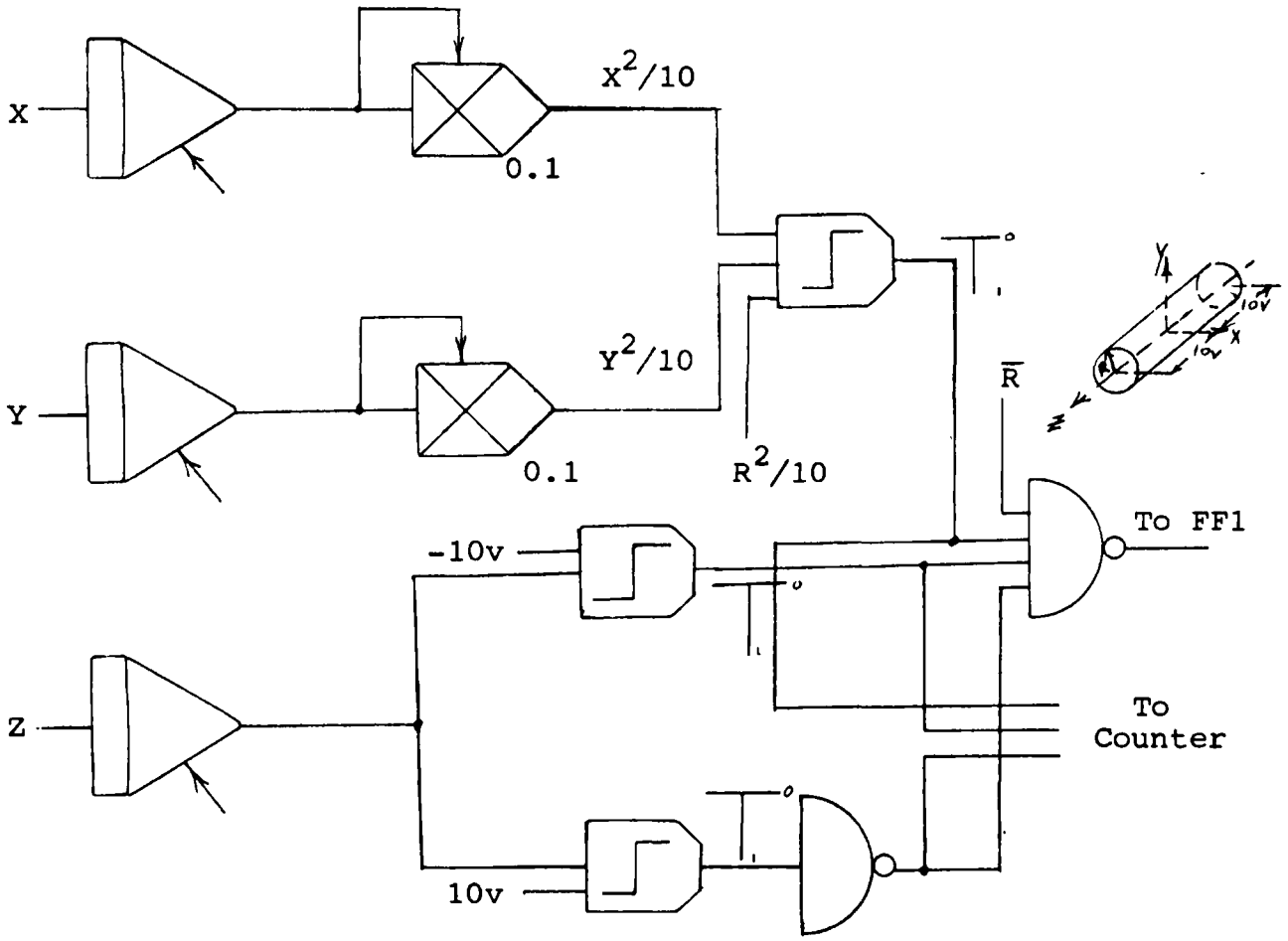

Figure 3. Extension of Example Problem to Two- and Three-Dimensional Problems

EXPERIMENTS WITH VARIOUS BOUNDARIES

Experimental Design

Proper utilization of our eigenvalue estimates, given by Eq. (19), depends upon the correct choice of t_1 and Δt and hence on the choice of T_1, ΔT, and on our random step size "y".[7] The sensitivity of the estimate to variations in random walk source point and to dimensional boundary changes should also be determined if the estimate is to apply to the determination of lowest eigenvalues for boundaries of any shape and size.

Since time increments, step size, and possibly random walk starting point are all correlated, two initial choices were made:

1) Start all random walks from a point more or less centered with respect to the boundary.
2) Choose a step size of 0.5 volts, based on a 20 volt ($\pm$ 10) boundary in all directions.

The criterion employed in initially selecting ΔT was to choose a ΔT covering the largest percent change in N_t while remaining within existing computer time limits. Figure 4, which is a plot of N_t vs. $T = t/DG^2$ for a one-dimensional boundary, was utilized in making an initial decision. Also included in Fig. 4 is a plot for the curve $e^{-\lambda^1 T}$, where λ^1 is the true eigenvalue. As expected, the curves agree quite closely. Trial of several combinations

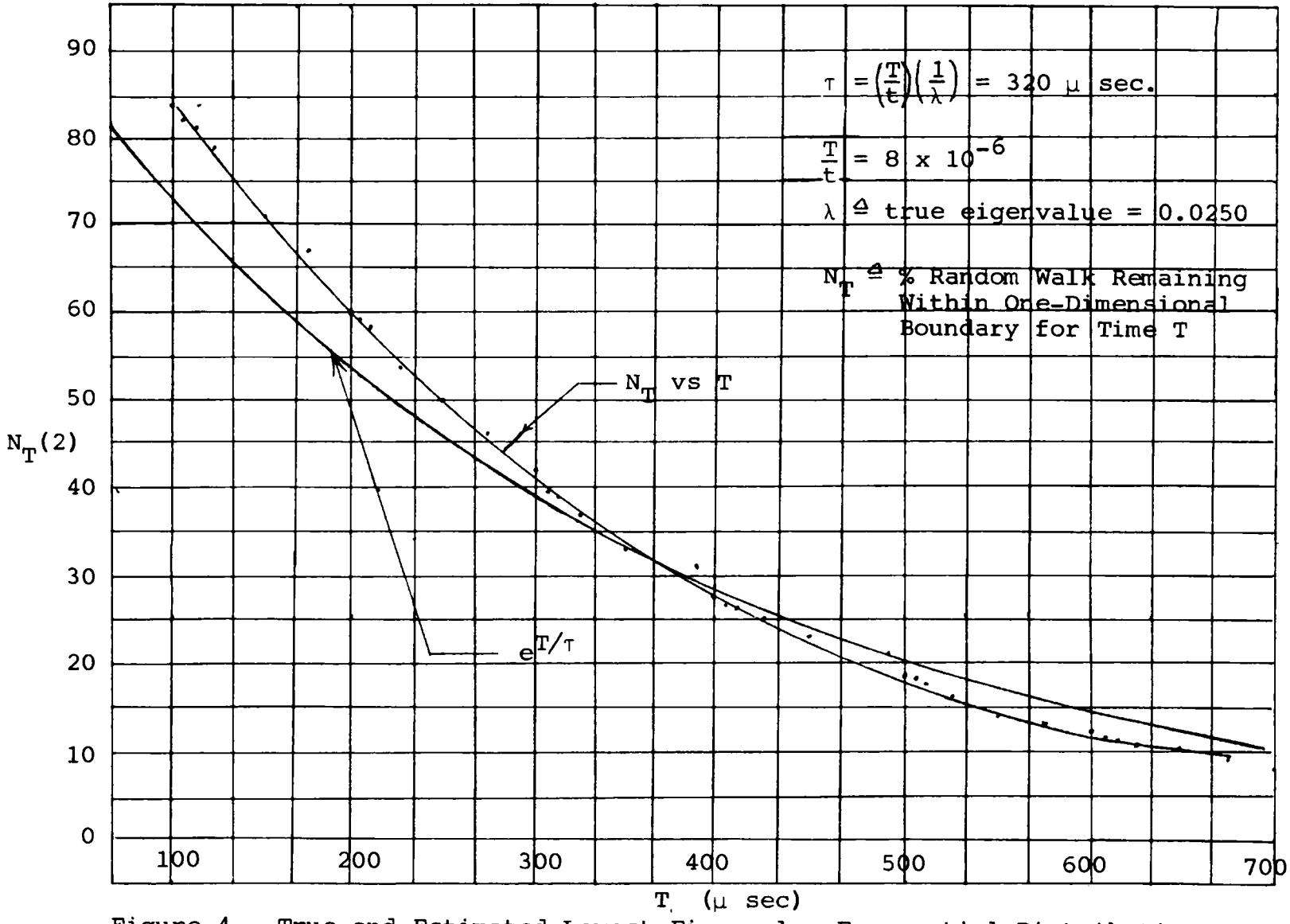

Figure 4. True and Estimated Lowest Eigenvalue Exponential Distributions

of T_1 and ΔT yielded T_1 = 125 μ sec. and T_2 = 525 μ sec. as values which produced the best estimate for our one dimensional boundary. These values were also chosen to represent all T values in two and three dimensions in the $\pm$ 10 volts bounded, 0.5 volt step size, cases.

Statistically, the estimated eigenvalue "$\hat{\lambda}$" converges to the true eigenvalue according to the approximations on page 40 and within the circle of convergence described by Wasow[17] as the sample size "N" increases.

ASTRAC II enables the user to take up to 1,000 walks/second with fast multipliers, comparators, and digital logic to accomodate this high repetition rate. One sample consisted of 10,000 tallied walks, thus taking full advantage of ASTRAC II's speed while assuring statistical convergence.

Parameters, Estimates and Errors

The boundaries considered in this paper and their corresponding true eigenvalues are tabulated in Table 1. The parameters, final estimates, and associated errors for each boundary are shown in the fixed tabular block forms given below. The one-dimensional boundary is given special treatment in that graphs indicating the eigenvalue estimate's probability density distribution and the effect on the estimated value due to variations in the random walk source point are presented. Also, the terminology used in all tabular blocks will be presented here.

Table 1. Various Boundaries and Corresponding Lowest Eigenvalues

1. One-Dimensional Boundary 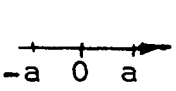 $\lambda_t^1 = \left(\frac{\pi}{2a}\right)^2$ $\lambda_t^1 = .024674$ for a = 10v	2. Circular Boundary 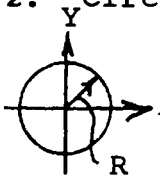 $\lambda_t^1 = \left(\frac{2.4048}{R}\right)^2$ $\lambda_t^1 = .057830$ for R = 10
3. Square Boundary 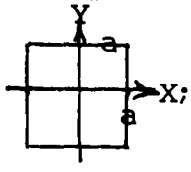 $\lambda_t = 2\left(\frac{\pi}{2a}\right)^2$ $\lambda_t^1 = .049348$ for a = 10	4. Rectangular Boundary 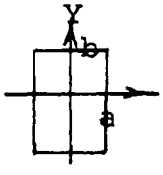 $\lambda_t^1 = \left(\frac{\pi}{2a}\right)^2 + \left(\frac{\pi}{2b}\right)^2$ $\lambda_t^1 = .063227$ for a = 8, b = 10
5. Vaned Circular Boundary 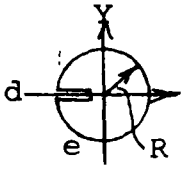 See Reference 16 for true lowest eigenvalue $\lambda_t^1 = 0.04678$ for R = 10	6. Spherical Boundary 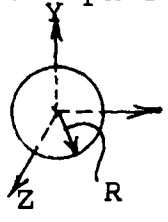 $\lambda_t^1 = \left(\frac{3.14159}{R}\right)^2$ $\lambda_t^1 = .098696$ for R = 10
7. Cubical Boundary 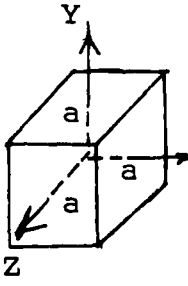 $\lambda_t^1 = 3\left(\frac{\pi}{2a}\right)^2$ $\lambda_t^1 = .074022$ for a = 10	8. Cylindrical Boundary 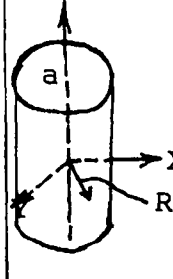 $\lambda_t^1 = \left(\frac{2.4048}{R}\right)^2 + \left(\frac{\pi}{2a}\right)^2$ $\lambda_t^1 = .082504$ for R = 10, a = 10

Numerical Parameters, Results and Errors

1. One Dimensional Boundary or Vibrating String

$T_1 = 125\ \mu$ sec N = 10,000 walks

$T_2 = 525\ \mu$ sec f_R = 1000 walks/sec

$\Delta T = 400\ \mu$ sec t/T = 0.125×10^6

$y = 0.5$ volts/μ sec $f_{noise\ clock}$ = 1 MHz

$\hat{\lambda}^1_{29} = 0.0277$ for $y_o = 0$

$S^2 = 4.65 \times 10^{-6}$

$S = 2.16 \times 10^{-3}$

$\epsilon = 12.15\%$

where: (1) $\hat{\lambda}^1_m$ is the estimated eigenvalue based on m samples of 10,000 walks each

(2) S^2 is the sample variance $S^2 = \overline{(\hat{\lambda}^1_m)^2} - \overline{(\hat{\lambda}^1_m)}^2$

(3) S is the sample standard deviation $S = \sqrt{S^2}$

(4) ϵ is the error of the estimated eigenvalue from its true value.

$$\epsilon = \frac{|\lambda^1_t - \hat{\lambda}^1_m|}{\lambda^1_t}$$

In addition to the above results, Figs. 5 and 6 indicate the normally distributed density of the estimated eigenvalue, and the variation in the estimate with changes

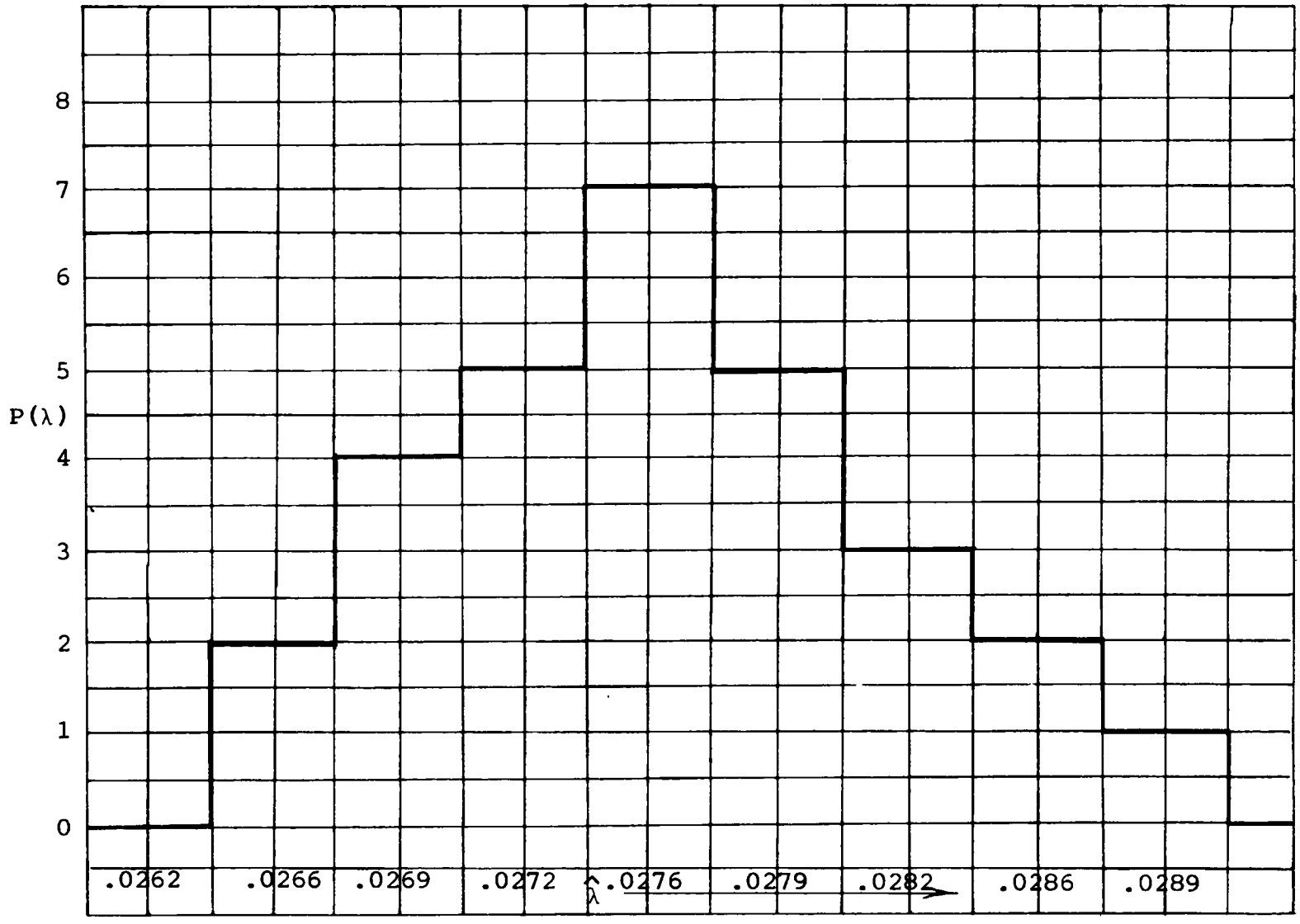

Figure 5. Sample Probability Density Distribution for Vibrating String Problem

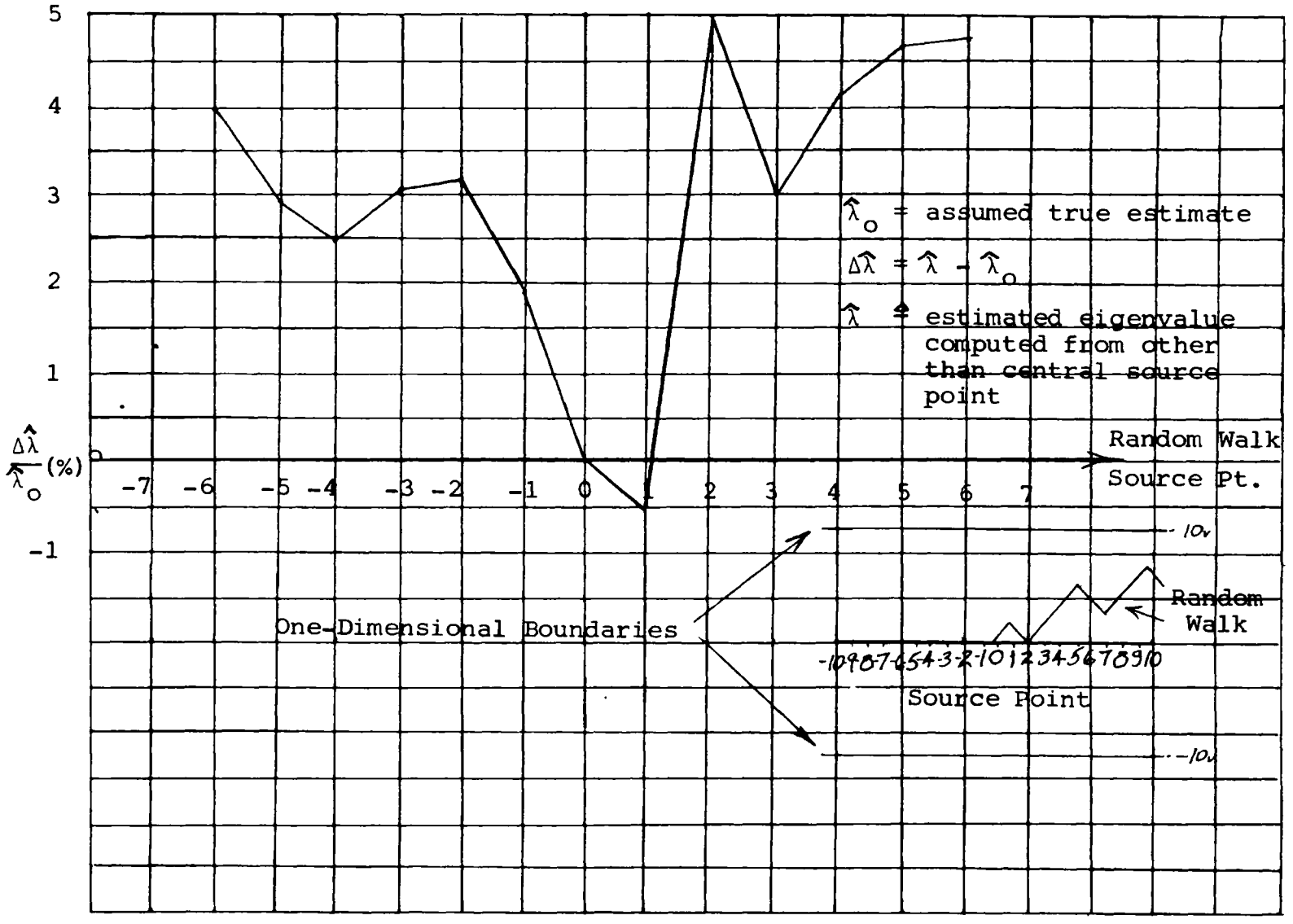

Figure 6. Sensitivity of Estimate to Variations in the Walk Source Point

in the walk source point, respectively. Although only 29 eigenvalues were estimated, Fig. 5 does indeed indicate an approximately normal distribution with mean range including the true mean eigenvalue. Figure 6 indicates that all sample eigenvalues are geometrically insensitive, i.e., less that 5% statistical error from true value, to initial random walk point variations within $\pm$ 60% from midpoint to boundary. Beyond $\pm$ 60%, the estimates became progressively inaccurate due to the failure of the circuitry to record a hit and reset the integrator at the rapid rate at which the boundary hits occurred.

2. Two Dimensional Circular Boundary

$T_1 = 125\ \mu$ sec N = 10,000 walks

$T_2 = 525\ \mu$ sec f_R = 1,000 walks/sec

$\Delta T = 400\ \mu$ sec $t/T = 0.125 \times 10^6$

$y = 0.5$ volt/μ sec $f_{\substack{noise \\ clock}} = 1$ MHz

$\hat{\lambda}_5^1 = 0.0514$ for $(x_o, y_o) = (0,0)$

$S^2 = 1.85 \times 10^{-7}$

$S = 4.30 \times 10^{-4}$

$\varepsilon = 11.06\%$

For $\hat{\lambda}_5^1$ originating at $x_o = 0$; $y_o = 0.5$, 1, 2, 3, 4, 5 and 6 volts, no error from estimated value at (0,0) greater than 1.5% was recorded. See Fig. 7A for photograph of walks within this boundary.

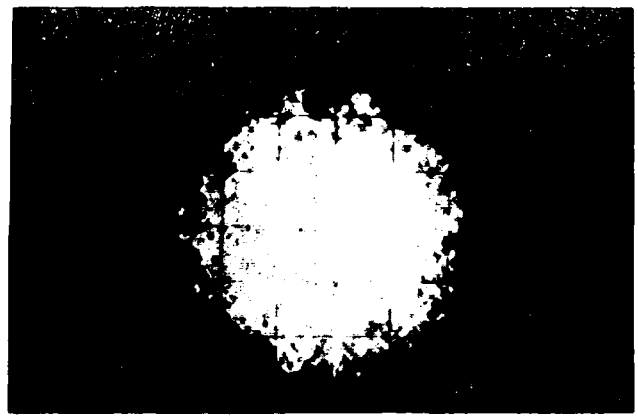

(a)

(b)

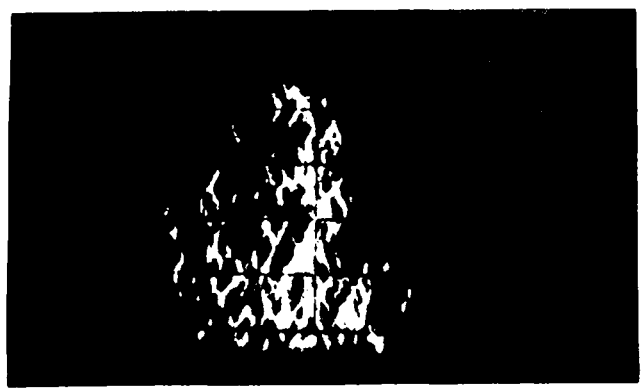

(c)

Figure 7. Photographs of Random Walks within (a) Circular, (b) Rectangular and (c) Triangular Boundaries

3. Two Dimensional Square Boundary

T_1 = 125 μ sec N = 10,000 walks

T_2 = 525 μ sec f_R = 1,000 walks/sec

ΔT = 400 μ sec $t/T = 0.125 \times 10^6$

y = 0.5 volts/μ sec $f_{noise\ clock}$ = 1 MHz

$\hat{\lambda}_5^1$ = 0.0477 at $(x_o, y_o) = (0,0)$

ϵ = 3.24%

For $\hat{\lambda}_5^1$ originating at $x_o = 0$; $y_o = \pm .5, \pm 1, \pm 3, \pm 5$ volts and $x_o = y_o = \pm .5, \pm 1, \pm 2, \pm 3$ volts

No error from estimated value at (0,0) greater than 3.45% was recorded.

4. Two Dimensional Rectangular Boundary

T_1 = 125 μ sec N = 10,000 walks

T_2 = 525 μ sec f_R = 1,000 walks/sec

ΔT = 400 μ sec $t/T = 0.125 \times 10^6$

y = 0.5 volts/μ sec $f_{noise\ clock}$ = 1 MHz

$\hat{\lambda}_5^1$ = 0.0535 at $(x_o, y_o) = (0,0)$

ϵ = 15.20%

For $\hat{\lambda}_5^1$ originating at (2,1.5) an error of 2.9% from estimate at (0,0) was recorded. See Fig. 7B for photograph of walks within this boundary.

5. Two Dimensional Circular Boundary with One Vane

T_1 = 1250 μ sec N = 10,000 walks

T_2 = 5250 μ sec f_R = 1,000 walks/sec

ΔT = 400 μ sec $t/T = 0.125 \times 10^7$

y = 0.5 volts/10 μ sec f_{noise}^{clock} = 100 KHz

$\hat{\lambda}_5^1 = 0.0501$ at $(x_o, y_o) = (1,0)$

ϵ = 9.05%

6. Three Dimensoinal Spherical Boundary

T_1 = 125 μ sec N = 10,000 walks

T_2 = 525 μ sec f_R = 1,000 walks/sec

ΔT = 400 μ sec $t/T = 0.0625 \times 10^6$

y* = 0.5 volts/2 μ sec f_{noise}^{clock} = 0.5 MHz

$\hat{\lambda}_5^1 = 0.1033$ for $(x_o, y_o, z_o) = (0,0,0)$

ϵ = 4.66%

For $\hat{\lambda}_5^1$ originating at (1,1,1) an error of 2.22% from estimate at (0,0,0) was recorded.

*Here an integrator input resistance equal to 2K rather than the normally used 1K input resistor was employed.

7. Three Dimensional Cubical Boundary

T_1 = 125 μ sec N = 10,000 walks

T_2 = 525 μ sec f_R = 1,000 walks/sec

ΔT = 400 μ sec $t/T = 0.0625 \times 10^6$

y^* = 0.5 volts/2 μ sec f_{noise} = 0.5 MHz

$\hat{\lambda}_5^1 = 0.0629$ for $(x_o, y_o, z_o) = (0,0,0)$ clock

ϵ = 14.99%

For $\hat{\lambda}_5^1$ originating at (1,1,1) an error of 0.235% from estimate at (0,0,0) was recorded.

8. Three Dimensional Cylindrical Boundary

T_1 = 200 μ sec N = 10,000 walks

T_2 = 800 μ sec f_R = 1,000 walks/sec

ΔT = 600 μ sec $t/T = 0.0625 \times 10^6$

y = 0.5 volts/2 μ sec f_{noise} = 0.5 MHz

$\hat{\lambda}_5^1 = 0.0786$ for $(x_o, y_o, z_o) = (0,0,0)$ clock

ϵ = 4.73%

For $\hat{\lambda}_5^1$ with walk originating at (1,1,1) an error of 0.259% from estimate at (0,0,0) was recorded.

*Here an integrator input resistance equal to 2K rather than the normally used 1K input resistor was employed.

ERROR SOURCES

Estimate Approximation Error

Our lowest eigenvalue estimate, repeated here for convenience,

$$\hat{\lambda}^1 = \frac{\ln \frac{N_{t_1}}{N_{t_2}}}{t_2 - t_1}$$

is based on the assumption that both t_1 and t_2 are large, thus enabling the higher order eigenvalue exponentials to approach zero.[7] With our values of t_1 = 15.625 sec and t_2 = 65.625 sec this error is negligible.

Equipment Considerations

The ASTRAC II noise source has a bandwidth of 500 KHz which, compared to the 30 MHz bandwidth of the amplifiers, is the band limiting device in our study. The white-noise assumption is, however, valid for sufficiently long steps (i.e., by increasing G) thus insuring independence between steps and hence randomness.

At the very start of the random walks, the mean or d.c. component of the random noise source is not properly filtered out by the slowly charging 10 μf capacitor. Although this initial charging time could lead to erroneous biased random walks, it was easily overcome by merely

running the computer until the capacitor was fully charged, prior to any recordings.

Amplifier drift errors were kept below 1% of 10v. (100 mv) by ensuring that the offset voltage K satisfied:

$$K \leq 2DnG \times 10^{-3} \tag{20}$$

Notice for f_R = 1000 runs/sec and $f_{noise\ clock}$ = 1 MHz or for f_R = 100 runs/sec and $f_{noise\ clock}$ = 100 KHz with R_{input} = 1K in both cases, the value for 2DnG is 3.0. For the amplifiers used in ASTRAC II, $K \leq 20 \times 10^{-5}$, which is well within the conditions of Eq. (20).

The comparators and logic must respond fast enough to record a boundary hit and to reset all integrators before another step occurs. ASTRAC II's fast comparators and logic do indeed accomplish this feat within less than 1 μ sec, within the smallest possible time for a step with the fastest noise-clock frequency of 1 MHz.

Because comparator static hysteresis (10 millivolts) requires a boundary absorption rather than just a hit for detection, a boundary hit for a one-dimensional boundary has a small probability

$$\left[1 - \sum_{i=1}^{N} \binom{i}{\frac{i+1}{2}} \left(\frac{1}{2}\right)^i\right]$$

where 1) i is always odd and $\leq$ N and
2) $N = t/T_{noise\ clock}$

of not crossing the boundary in time "t" remaining after a boundary hit, and thus boundaries are defined only within $\pm$ 10 mv. This applies to multi-dimensional boundaries as well.

As expected, and illustrated in Fig. 8, errors resulting from small, random step sizes exist due to the increasing dominance of computer drift, while truncation errors become significant as larger step sizes are employed. Also, the small number of binary distributed random step events tallied over our fixed time interval results in a poor binomial approximation to a normal distribution. This last error may be reduced by choosing T_1 = (0.5/x) 125 μ sec. and T_2 = (0.5/x) 525 μ seconds.

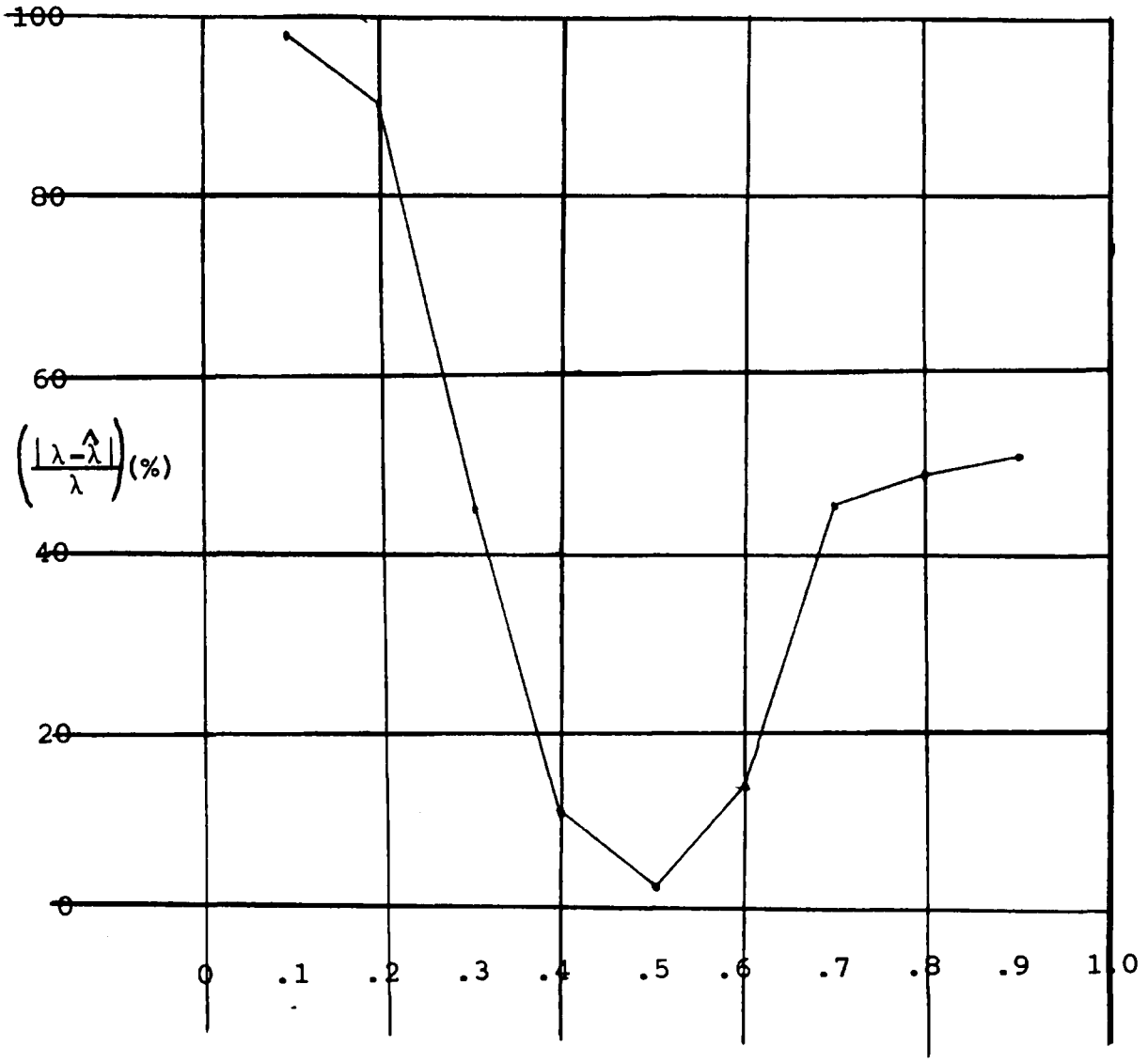

Figure 8. Sensitivity of Estimate to Variations in Random Walk Step Size

APPLICATIONS

As mentioned previously, the partial differential equations considered may describe a variety of physical processes including the vibration of a string or two-dimensional membrane, or the motion of electromagnetic waves in a waveguide or of neutrons in a nuclear plant.

The first application concerns the determination of cutoff frequencies of waveguides. Although applicable to waveguides of any cross-sectional contour, this Monte Carlo technique compares with, and in some ways surpasses, other techniques when applied to cross-sectional contours for which closed form solutions obtained through classical methods are non-existent. The importance of this application may be observed by noting the operational advantages in employing an arbitrarily contoured cross-sectional waveguide.[2]

The propagation of an electromagnetic wave in a waveguide in an axial direction as shown in Fig. 9 is mathematically represented by Helmholtz's partial differential equation:

$$\nabla^2 \psi(x,y) + K_i^2 \psi(x,y) = 0$$

where: $\psi(x,y)$ is the potential function

∇^2 is the two-dimensional Laplacian Operator

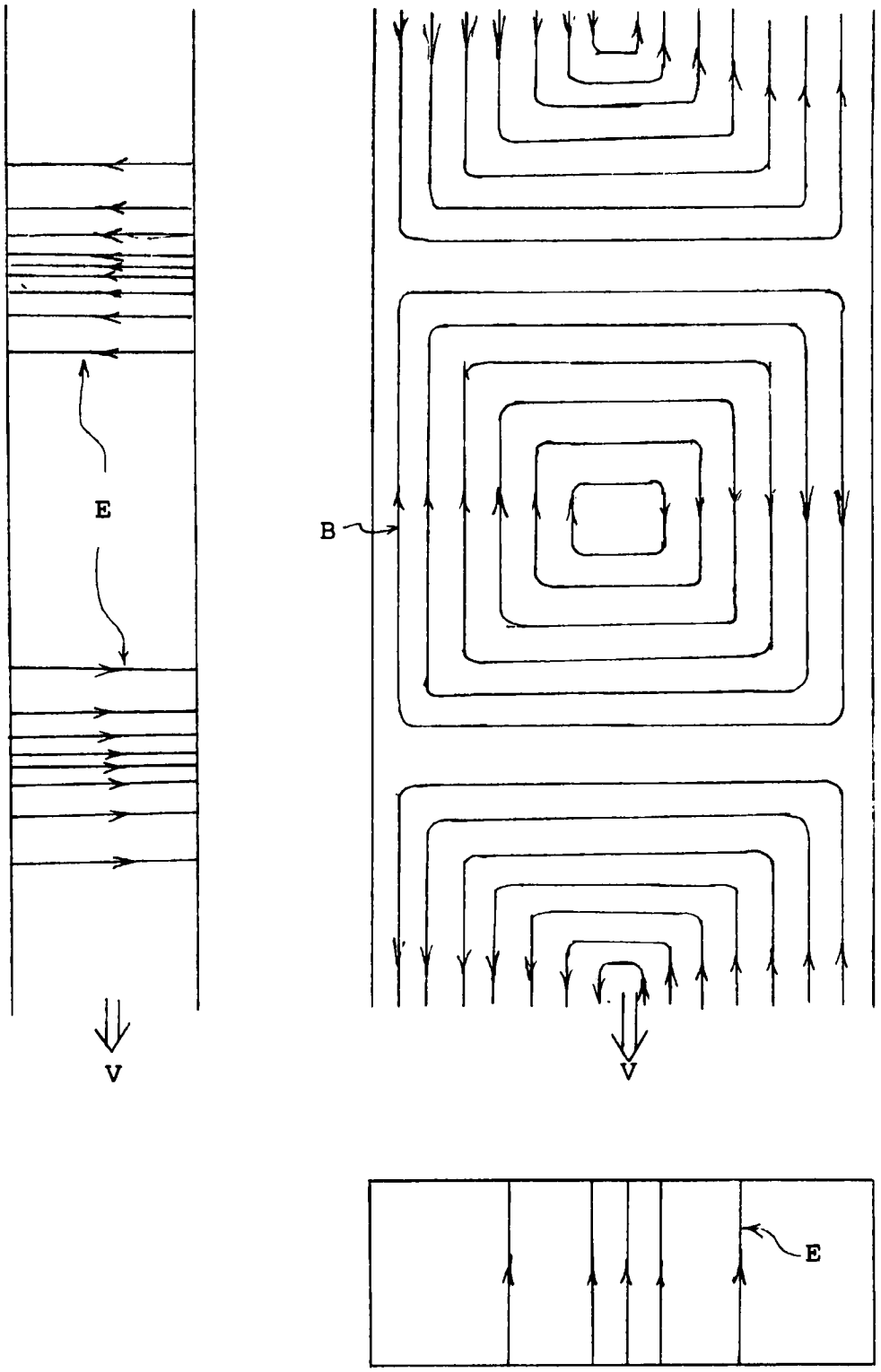

Figure 9. Electromagnetic Wave Propagating in Waveguide

K_i's are real discrete wave numbers containing cutoff frequencies analytically given as:

$$K_i^2 = K_o^3 - K_z^2$$

$$K_o^2 = \omega^2 \mu_o \epsilon_o$$

$$K_z^2 = 2\pi/\lambda_g^{(i)}$$

$\lambda_g^{(i)}$ defined as the waveguide wavelength of the i^{th} mode

In the T.M. wave mode $\psi[L(x,y)] = 0$ where $L(x,y) = 0$ is the waveguide cross-section boundary equation.

The solution of the wave equation with the above boundary condition for the lowest wave number K_1 may be accomplished through utilization of the Monte Carlo technique and in fact yields the eigenvalue describing the first mode of vibration of the two-dimensional membrane described by the wave equation.

A second application concerns the criticality problem associated with nuclear reactors.[9] The criticality problem asks whether a pulse of neutrons when injected into a nuclear reactor assembly will cause a multiplying chain reaction or will merely by absorbed. More specifically, it is concerned with the size of the assembly at which reaction is just able to sustain itself.

The criticality constant defining a subcritical, critical or supercritical combination reactor assembly and

absorbent material can be determined by making a simple comparison between a directly measurable quantity known as the material buckling coefficient and the geometric buckling coefficient B_{g_i}.[4] B_{g_i} is mathematically given by:[8]

$$B_{g_i}^2 = \frac{-\nabla^2 R(\bar{r})}{R(\bar{r})}$$

or as:

$$\nabla^2 R(\bar{r}) + B_{g_i}^2 R(\bar{r}) = 0$$

where: $R(\bar{r})$ describes the neutron flux density at coordinate position $\bar{r}$.

∇^2 is the three-dimensional Laplacian operator.

The criticality problem is indeed an eigenvalue problem as we recognize that the solution of the above standing-wave equation for B_{g_1} yields the eigenvalue describing the first mode of vibration of the three-dimensional body.

Just as the lowest eigenvalue solutions to the partial differential equations describing motion of membranes are subject to the boundary conditions that the edges of the membranes are in a fixed position, so too are the buckling coefficient solutions to the partial differential equations describing the neutron density distribution in an operating reactor subject to the boundary condition

that the flux must approach zero along the boundary of the reactor.[4]

CONCLUSION

The feasibility of a Monte Carlo method applied toward the estimation of lowest eigenvalues of partial differential equations has been demonstrated. The accuracy of all eight estimates (< 16 percent) appear to satisfy engineering needs where close approximations are usually sufficient.

The availability of fast-repetitive analog computers such as ASTRAC II makes this method potentially attractive. With these computers, we are able to solve partial differential equations for their lowest eigenvalues with, as compared to current methods, a minimum amount of computation time. This is especially attractive for multidimensional problems.

APPENDIX A

DERIVATION OF LOWEST EIGENVALUE ESTIMATE

This appendix describes the theory which yields the lowest eigenvalue of boundary value problems.

Consider the following problem,

$$L_{\bar{r}}\, U(\bar{r}) + k^2 U(\bar{r}) = 0 \qquad \text{(A.1)}$$

where $U(\bar{r})$ is defined within a bounded region R. On the boundary C, of R, the function $U_c(\bar{r}_b)$ is defined to be zero. The non-trivial solutions of (A.1) which satisfy this boundary condition are called the eigenfunctions of the problem, and the corresponding values of k^2 are, the eigenvalues. The problem is to formulate a Monte Carlo procedure to calculate the lowest eigenvalue of (A.1). It will be assumed that the differential operator is such that:

a) the eigenvalues k^2, are real (L is Hermitian)

b) the operator L will yield a discrete set rather than a continuous spectrum of eigenvalues.

The generalized time invariant operator L(r) is given below for an n dimensional space.

$$L(\bar{r})U(\bar{r}) = -\sum_i \frac{\partial}{\partial r_i} C_i(\bar{r})U(\bar{r}) + \frac{1}{2}\sum_{j\ell} \frac{\partial^2}{r_j r_\ell}\left[D_{j\ell}(\bar{r})U(\bar{r})\right] \qquad \text{(A.2)}$$

Conceptually, it is perhaps easiest to discuss this problem in two dimensions; however, the procedure holds for n dimensions providing that the region R and its boundary are properly defined.

Consider a two-dimensional random walk originating at an interior point (x_o, y_o) of R. Let $Q(x_o, y_o, t)$ denote the probability that the particle will not be absorbed (stay within the boundary) in a time t given that the walk starts at a time t = 0.

Now,

$$Q(x_o, y_o, t) = \int_R \int p(x, y, t/x_o, y_o)\, dxdy \qquad (A.3)$$

where $p(x, y, t/x_o, y_o)$ represents the probability density that at time t the particle performing the random walk is at point (x,y) given that it originated at (x_o, y_o). Integration over the entire region R produces the probability that the particle remains within the absorbing boundary C.

Since we are dealing with a Markov process (by assumption), the conditional density function $p(x, y, t/x_o, y_o)$ satisfies Kolmogorov's forward partial differential equation.[6,12,18]

$$\frac{\partial}{\partial t} p(x, y, t/x_o, y_o) = L_{x,y}\, p(x, y, t/x_o, y_o) \qquad (A.4)$$

with the following conditions:

$$p(x, y, t/x_o, y_o) = 0 \text{ on } C \text{ for } t \neq 0$$

i.e., the boundary is an absorbing one

$$p(x,y,t/x_o,y_o) \longrightarrow \delta(x-x_o)\delta(y-y_o) \text{ as } t \to 0$$

where δ denotes the Dirac delta function.

The general form of equation (A.4) is the following

$$\frac{\partial}{\partial t} p(\bar{r},t/\bar{r}_o,t_o) = -\sum \frac{\partial}{\partial r_i}\left[C_i(\bar{r},t)p(\bar{r},t/\bar{r}_o,t_o)\right] + \frac{1}{2}\sum \frac{\partial^2}{\partial r_m \partial r_\ell}\left[D_{m,\ell}(\bar{r})p(\bar{r},t/\bar{r}_o,t_o)\right] \quad (A.5)$$

where the terms $C_i(\bar{r})$ and $D_{m,\ell}(\bar{r})$ are obtained from the generalized Langevin equations given below. Considering a three dimensional case, $r_1 = x$, $r_2 = y$, $r_3 = z$, we have

$$\frac{dx}{dt} + A_1(x,y,z,t) = B_1(x,y,z,t)N_1(t) \quad (A.6)$$

$$\frac{dy}{dt} + A_2(x,y,z,t) = B_2(x,y,z,t)N_2(t) \quad (A.7)$$

$$\frac{dz}{dt} + A_3(x,y,z,t) = B_3(x,y,z,t)N_3(t) \quad (A.8)$$

It is assumed that both A_i and B_i vary slowly with time when compared to the rapid variations of $N_i(t)$. The noise terms $N_i(t)$ are uncorrelated stationary white gaussian noise sources with zero mean and power spectral density $2Dn_i$.

The relationship between the coefficients of the Langevin equations and the terms in the operator $L(\bar{r})$ is given by

$$C_1(\bar{r},t) = -A_1(\bar{r},t) \quad (A.9)$$

$$C_2(\bar{r},t) = -A_2(\bar{r},t) \tag{A.10}$$

$$C_3(\bar{r},t) = -A_3(\bar{r},t) \tag{A.11}$$

$$D_{11}(\bar{r},t) = 2Dn_1B_1^2(\bar{r},t) \tag{A.12}$$

$$D_{22}(\bar{r},t) = 2Dn_2B_2^2(\bar{r},t) \tag{A.13}$$

$$D_{33}(\bar{r},t) = 2Dn_3B_3^2(\bar{r},t) \tag{A.14}$$

$$D_{12} = D_{13} = D_{23} = 0 \tag{A.15}$$

If the operator L_{xy} in Eq. (A.4) is of such a nature that the method of separation of variables can be applied to the partial differential equation, then we assume that

$$p = T(t)U(x,y) \tag{A.16}$$

Substitution in Eq. (A.4) yields

$$T'(t)U(x,y) = T(t)L_{x,y}U(x,y) \tag{A.17}$$

Division of both sides of the above equation by $T(t)U(x,y)$ gives

$$\frac{T'(t)}{T(t)} = \frac{L_{xy}U(x,y)}{U(x,y)} \tag{A.18}$$

Since the space coordinates do not appear in the left hand side and time does not appear in the right hand side, both sides of the equation are set equal to a constant, $-k^2$

$$\frac{T'(t)}{T(t)} = -k^2 \tag{A.19}$$

Eq. (A.19) yields solutions of the form

$$T(t) = \exp(-k^2 t) \tag{A.20}$$

The other equation which results from this technique is

$$L_{x,y}U(x,y) + k^2 U(x,y) = 0 \tag{A.21}$$

Where $U(x,y)$ is zero for (x,y) on the boundary, which results from the condition that $p(x,y,t/x_o,y_o) = 0$ on the boundary. Equation (A.21) along with the boundary conditions yields a set of orthonormal functions, $\psi_j(x,y)$ corresponding to values of $k = k_j$.

Since L is Hermitian, the solution to Eq. (A.4) can be written in series form in terms of the eigenvalues and orthogonal eigenfunctions as,

$$p(x,y,t/x_o,y_o) = \sum_{j=1}^{\infty} A_j e^{-k_j^2 t} \psi_j(x,y) \tag{A.22}$$

Where the k_j's are assumed to be an increasing discrete set of real numbers.

Using the initial conditions on the conditional density function $p(x,y,t/x_o,y_o) \longrightarrow \delta(x-x_o)\delta(y-y_o)$ as $t \to 0$ Eq. (A.22) may be written as

$$\delta(x-x_o)\delta(y-y_o) = \sum_{j=1}^{\infty} A_j \psi_j(x,y) \tag{A.23}$$

Multiplying both sides of the above equation by $\psi_m(x,y)$ and integrating over R

$$\int_R \int \psi_m(x,y)\delta(x-x_o)\delta(y-y_o)\,dxdy$$

$$= \int_R \int \sum_{j=1}^{\infty} A_j \psi_j(x,y)\psi_m(x,y)\,dxdy \qquad (A.24)$$

If the series representation of the conditional density function, Eq. (A.22), is uniformly convergent then the order of integration and summation can be interchanged, resulting in the following equation:

$$\psi_k(x_o,y_o) = \sum_{j=1}^{\infty} A_j \int_R \int \psi_j(x,y)\psi_k(x,y)\,dxdy \qquad (A.25)$$

Since the ψ_k's are an orthonormal set, $\psi_k(x_o,y_o) = A_k$, and Eq. (A.22) can now be written in the form,

$$p(x,y,t/x_o,y_o) = \sum_{j=1}^{\infty} e^{-k_j^2 t} \psi_j(x_o,y_o)\psi_j(x,y) \qquad (A.26)$$

Substitution of this expression into Eq. (A.3) yields

$$Q(x_o,y_o,t) = \int_R \int \sum_{j=1}^{\infty} e^{-k_j^2 t} \psi_j(x_o,y_o)\psi_j(x,y)\,dxdy \qquad (A.27)$$

$$Q(x_o,y_o,t) = \sum_{j=1}^{\infty} e^{-k_j^2 t} \psi_j(x_o,y_o) \int_R \int \psi_j(x,y)\,dxdy \qquad (A.28)$$

If $\int_R \int \psi_j(x,y)\,dxdy = B_j$ then

$$Q(x_o,y_o,t) = \sum_{j=1}^{\infty} e^{-k_j^2 t} \psi_j(x_o,y_o) B_j \qquad (A.29)$$

Expanding the series,

$$Q(x_o,y_o,t) = e^{-k_1^2 t} \psi_1(x_o,y_o) B_1 + e^{-k_2^2 t} \psi_2(x_o,y_o) B_2$$

$$+ \ldots\ldots\ldots \qquad (A.30)$$

Since the k's are an increasing set of real numbers, for large values of time, the first term of the series is the only significant term and Eq. (A.30) may be written as follows:

$$Q(x_o,y_o,t) \approx e^{-k_1^2 t} \psi_1(x_o,y_o) B_1$$

Taking logarithms of both sides of the equation yields,

$$k_1^2 = \frac{-\ln Q(x_o,y_o,t)}{t} + \frac{\ln \psi_1(x_o,y_o) B_1}{t} \qquad (A.32)$$

Taking the limit as $t \to \infty$

$$k_1^2 = \lim_{t\to\infty} \frac{-\ln Q(x_o, y_o, t)}{t} \tag{A.33}$$

When finite time t, is involved, the calculation of the lowest eigenvalue of Eq. (A.1) by means of Eq. (A.33) is subject to two sources of error. The first is due to neglecting all the terms in the series representation, Eq. (A.29), after the initial one and the second source of error results from neglecting the quantity $\frac{\ln \psi_1(x_o, y_o) B_1}{t}$ for the finite values of time since in any computational scheme a finite value of time must be employed. This latter source of error is removed by the following procedure:

Consider Eq. (A.30) for two large values of time t_1 and t_2, i.e.:

$$Q(x_o, y_o, t) = e^{-k_1^2 t_1} \psi_1(x_o, y_o) B_1 \tag{A.34}$$

$$Q(x_o, y_o, t) = e^{-k_1^2 t_2} \psi_1(x_o, y_o) B_1 \tag{A.35}$$

Dividing Eq. (A.35) by Eq. (A.34), one obtains

$$\frac{Q(x_o, y_o, t_2)}{Q(x_o, y_o, t_1)} = e^{-k_1^2 (t_2 - t_1)} \tag{A.36}$$

Taking logarithms again yields

$$k_1^2 = \frac{\ln Q(x_o, y_o, t_1) - \ln Q(x_o, y_o, t_2)}{t_2 - t_1} \tag{A.37}$$

The quantity $Q(x_o, y_o, t)$, representing the probability that a particle which begins a random walk at a point (x_o, y_o) will remain within an absorbing boundary C during the time interval t_1, can be approximated by the following sampling procedure.

Start a particle on a random walk from the point (x_o, y_o) at time t = 0. The rules governing the random walk are given by the generalized Langevin Eqs. (A.6), (A.7), and (A.8). The walk continues for a time t and at the end of this time interval the observation is made as to whether or not the particle has remained within the absorbing boundary C. Perform N_o such random walks and count the numbers of particles N_t which have not left the region during the time interval (0,t). $Q(x_o, y_o, t)$ can be approximated by

$$Q(x_o, y_o, t) \approx \frac{N_t}{N_o} \tag{A.38}$$

The lowest eigenvalue k_1^2 may now be calculated by the expression

$$k_1^2 = \frac{\ln \frac{N_{t_1}}{N_o} - \ln \frac{N_{t_2}}{N_o}}{t_2 - t_1} \qquad \text{(A.39)}$$

$$k_1^2 = \frac{\ln \frac{N_{t_1}}{N_{t_2}}}{t_2 - t_1} \qquad \text{(A.40)}$$

REFERENCES

1. Casarella, M. J. and P. A. Laura, "Determination of Cutoff Frequencies of Grooved Waveguides," Proceedings of the IEEE (Letters), Vol. 55, No. 6, June 1967, pp. 1096-1097.

2. Chi, M. and P. A. Laura, "Approximate method of determining the cutoff frequency of waveguides of arbitrary cross sections," IEEE Transactions, Microwave Theory and Techniques (Correspondence), Vol. M.T.T.-12, March 1964, pp. 248-249.

3. Dennemeyer, R., Introduction to Partial Differential Equations, McGraw-Hill, 1968.

4. Dessauer, G., "What is Buckling?", Nuclear News - ANS - September 1964, pp. 43-47.

5. Donsker, M. and M. Kac, "A Sampling Method for Determining the Lowest Eigenvalue and the Principal Eigenfunction of Schrodingers Equation," Journal of Research of the National Bureau of Standards, Vol. 44, May 1950, pp. 551-557.

6. Feller, W., An Introduction to Probability Theory and Its Applications, Second Edition, Vol. 1, Wiley, 1957.

7. Fortet, R., "On the Estimation of an Eigenvalue by an Additive Functional of a Stochastic Process, with Special Reference to the Donsker-Kac Method," Journal of Research of the National Bureau of Standards, Vol. 48, No. 1, January 1952, pp. 68-75.

8. Glasstone, S. and M. Edlund, The Elements of Nuclear Reactor Theory, Van Nostrund, New York, 1952, pp. 194-215.

9. Hammersley, J. M., and D. C. Handscomb, Monte Carlo Methods, "Methuen's Monographs on Applied Probability and Statistics," Wiley, New York, 1964, pp. 98, 99, 104-106.

10. Handler, H., High Speed Monte Carlo Technique for Hybrid-Computer Solution of Partial Differential Equations, PH.D. dissertation, Dept. of Electrical Engineering, University of Arizona, January 1967.

11. Korn, G. A., and T. M. Korn, Electronic Analog and Hybrid Computers, McGraw-Hill, New York, 1964.

12. Korn, G. A., and T. M. Korn, Mathematical Handbook for Scientists and Engineers, McGraw-Hill, New York, 1961.

13. Laura, P. A., "Application of the Point Matching Method in Waveguide Problems," IEEE Transactions on Microwave Theory (Correspondence), May 1966, Vol. M.T.T.-14, No. 5.

14. Laura, P. A., "A Simple Method for the Determination of Cutoff Frequencies of Waveguides with Arbitrary Cross Sections," Proceedings of the IEEE (Letters), Vol. 54, No. 10, October 1966, pp. 1495-1497.

15. Laura, P. A., "Determination of Cutoff Frequencies of Waveguides with Arbitrary Cross Sections by Point Matching," Proceedings of the IEEE (Correspondence), Vol. 53, No. 10, October 1965.

16. Little, W. D., and A. C. Soudack, "Boundary Generation and Detection in Random Walk Problems," Simulation, Vol. 7, No. 2, August 1966, pp. 63-65.

17. Wasow, W., "Random Walks and the Eigenvalues of Elliptic Difference Equations," Journal of the National Bureau of Standards, Vol. 46, No. 1, January 1951, pp. 65-73.

18. Wax, N., Selected Papers on Noise and Stochastic Processes, Dover, New York, 1954. Papers by Ming Chen Wang and G. E. Ohlenbeck.